DOI:10.18462/iir.hfo.2018.1128

PERFORMANCE OF AN OIL-FREE LINEAR COMPRESSOR USING R1234yf

Zhaohua Li, Kun Liang
Department of Engineering and Design, University of Sussex
Brighton, BN1 9QT, UK. zl282@sussex.ac.uk, kun.liang@sussex.ac.uk

ABSTRACT

As an alternative to the hydrocarbons (HCs), R1234yf synthetic refrigerant from the family of the hydrofluoroolefins (HFOs), has emerged recently as a replacement fluid for R134a. The purpose of this study is to investigate the performance of an oil-free linear compressor using R1234yf operated at different pressure ratios for household refrigerators. A mathematical model for the oil-free linear compressor using R1234yf has been developed. The compressor stroke was set as 14 mm for minimum dead volume with the evaporator temperature of – 23 °C. The result shows that the bleed flow rate can be 5% of main flow rate, and the resonant frequency varies between 32.7 Hz and 35.3 Hz for pressure ratios of 5-12. Cylinder mean pressure, shaft power, bleed flow, and clearance seal power loss increase with the pressure ratio. At pressure ratio of 10, and clearance seal power loss represents 8% of shaft power.

Keywords: Oil-free Linear Compressor, R1234yf, Resonant Frequency, Clearance Seal Power Loss, Bleed Flow

1. INTRODUCTION

For the last few decades, the application of chlorofluorocarbons (CFCs) can be wildly found in various refrigeration and air conditioning fields. However, CFCs can cause the destruction of the stratospheric ozone layer. For the concern of sustainable development, all F-gases with global warming potential (GWP) of more than 150 will be banned as the refrigerant or foam blowing agent in any hermetically sealed system from 2022. Because of the absence of chlorine in R1234yf, the ozone depletion potential (ODP) can be eliminated and the GWP can be minimised to 4 (2013). R1234yf has been regarded as an ideal next generation refrigerant for refrigeration and air conditioning industries. Several initial studies focused on the phase change of R1234yf. Richter et al., (2011) developed an equation of the p-ρ-T behaviour of R1234yf, covering the fluid region from T = (220 to 410) K with pressure up to 30 MPa. The most common commercially used refrigerant is R134a. Many works have been done on investigating the thermodynamic properties of R1234yf to compare their difference with those of R134a. This has been done to explore the possibility of R1234yf replacing R134a. Zillion et al., (2011) reported that enhancing 20% of the condenser and 10% of one of the evaporator face area could overtake the Coefficient of Performance (COP) value than the baseline R134a for equal cooling capacities. Lee and Jung (2012) examined R1234yf and R134a in a heat pump bench tester, and the experiment shows that these two refrigerants have similar thermodynamic properties and R1234fy can be used as an ideal replacement for mobile air-conditioners (MACs) with minor modifications. In addition, heat transfer coefficient is another attractive property for R1234yf. Col et al., (2010) pointed out that R1234yf displays lower heat transfer coefficients than R134a at the same operating conditions, but the preformation of pressure drop during two-phase flow at 40°C is 10% to 12% lower than R134a. To conclude, because of the low GWP, non-toxic and similar cooling capacity and energy efficiency to R134a, R1234yf is considered as an ideal replacement for R134a. However, cost of R1234yf is nearly 3 times higher than R134a and most important compatibility between R1234yf and R134a-based systems is the choice of lubricating oil. Since lubricating oil will reduce the heat transfer coefficient of vapour refrigeration system, particularly with compact heat exchangers, an oil-free system will allow the use of R1234yf especially for refrigerators with micro-channel heat exchangers, which have much lower refrigerant charge thus low cost and low emissions.

Regarding oil-free linear compressor for commercial refrigeration, Liang et al., (2014) pointed out that owing to the reduction of the crank and bearings, the mechanical friction losses could be reduced dramatically than that of the traditional reciprocating compressor. The overall efficiency of the linear compressor is about 20% higher than that of the crank-drive compressor. Liang et al., (2014) built a novel moving magnet linear compressor as shown in Fig. 1, which demonstrated that the motor efficiency could be improved to be over 90% with a revised motor design. Because of the structural superiority, the system efficiency can be improved significantly and a more compact structure can be achieved. In addition, as the absence of the oil in the loop, the pipe can be minimized to an extremely small scale without worrying about the stoppage of the pipe by oil. Therefore, linear compressor can be fabricated to a delicate scale that can be applied on the compact device and provide more space for refrigerator. In addition, as the removal of the crank, wear and tear can be limited to improve the reliability of the compressor. In this paper, a numerical model has been developed based on the prototype linear compressor and R1234yf to investigate the cylinder pressure, bleed flow rate, resonant frequency and power loss of the radial clearance with different pressure ratios. The simulation results will then be compared with experimental data for the linear compressor and R1234yf, which are currently being instrumented.

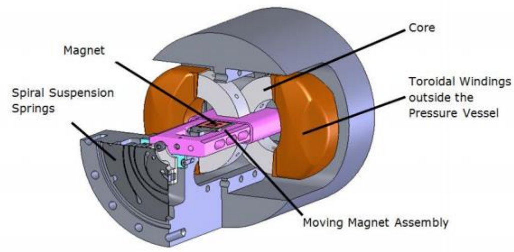

Figure 1 Prototype oil-free moving magnet linear compressor being instrumented

2. NUMERICAL MODELLING

2.1 System Layout

The proposed refrigeration system is shown in Fig.2. The system consists of two balanced oil-free linear compressors, a water-cooled condenser, an expansion valve, an evaporator, and a bleed flow loop. The hot and pressurised gaseous R1234yf is released from compressor to condenser. Between the two, a needle valve is added to control the pressure ratio. After that, R1234yf will flow to the evaporator and then goes back to the compressor and next cycle begins. An oil-free linear compressor tends to have a radial clearance (over 10 microns) to minimise the friction and to reduce the leakage. The leakage is caused by the radial clearance between piston and cylinder, which can result in power loss and piston offset (drift of piston mean position). To reduce the effect of radial clearance, a bleed flow loop with a needle valve control has been added to the system. The leaking R1234yf can return to the main flow from compressor body port, and the flow rate can be controlled by needle valve to keep the body pressure close to the compressor mean pressure.

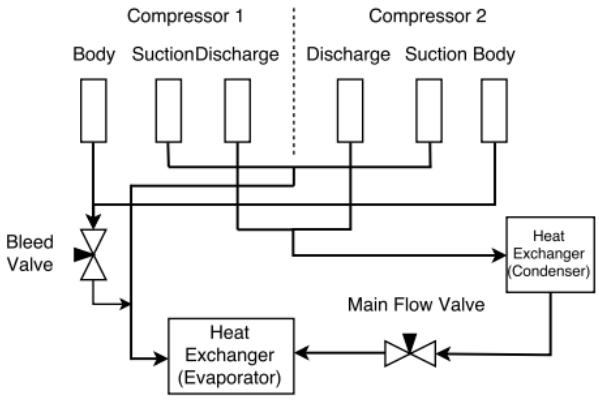

Figure 2 Schematic of the linear compressor test loop for R1234yf experiments

2.2 Overview and Assumption

Fig. 3 has illustrated the mathematical model of the system performance. The compression and expansion processes are considered as isentropic process. As the mathematical model has assumed an ideal reed valve for the linear compressor, pressure drop can be ignored. Based on the *P-V* diagram and the equations shown in Fig. 3, the bleed flow, power loss, shaft power, enthalpy and resonant frequency can be calculated. To reduce the piston offset and improve the compressor efficiency, the bleed flow and operating frequency can be adjusted.

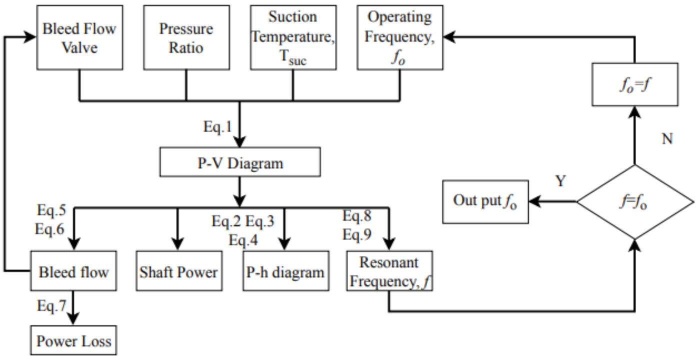

Figure 3 Flowchart of the mathematical model of the system performance using R1234yf

2.3 Pressure-Volume (*P-V*) Model

As has been mentioned in Lenz et al., (2002), the pressure-volume diagram can be plotted based on the adiabatic and isothermal process. The shaft work W_{shaft} is equal to the area of the pressure-volume loop. The dead volume can be calculated by the length of the compression chamber (15.6 mm) and piston stroke, which is equal to the minimum volume of the cylinder. The cylinder volume can be expressed as a cosine function of operating frequency and time. Each stroke is divided into 400 data points and the cylinder volume can be expressed by the average pressure of 400 data points as below

$$V = V_{\min} + \frac{S\pi D^2[\cos(2\pi f t)+1]}{8} \tag{1}$$

where f is the operating frequency, $V_{\min}$ is the minimum volume of cylinder, S is the piston stroke, and D is the piston diameter.

2.4 Pressure-Enthalpy (*P-h*) Model

The *P-h* diagram of an ideal vapour compression cycle for R1234yf as shown below is based on the pressure-enthalpy data from DuPont R1234yf refrigerant (2010). The discharge pressure and temperature can be derived from suction pressure and pressure ratio. From point 4' to point 1, extra heat is absorbed by refrigerant vapour from the environment, which makes the vapour temperature higher than its corresponding saturated vapour temperature. Refrigerant vapour becomes a superheated vapour. The superheated vapour will then be compressed by the free piston (1 - 2), which is the compression process; Then, the superheated vapour is discharged to the condenser and cooled to saturation temperature (2 – 2'). During the condensation process (2' - 3), saturation liquid is cooled from hot vapour. The cold liquid enters the expansion valve into the evaporator (2-3). As the expansion process is assumed to be an isenthalpic process, the cooled fluid can enter the evaporator without the change of enthalpy. The heat can be absorbed by low-pressure refrigerant liquid in the evaporator (4 – 4'). The mass flow rate for this operating condition is 2.27 g/s. Assuming the compression procession is isentropic, the enthalpy of refrigerant during different thermodynamic states throughout the refrigeration cycle can be determined by *P-h* diagram. The equation for isentropic power $\dot{W}_{isen}$ is shown below:

$$h_2 = \frac{\dot{W}_{isen}}{\dot{m}} + h_1 \tag{2}$$

where $\dot{m}$ is the mass flow rate of R1234yf and h is enthalpy.
By analysing the *P-h* diagram in Figure 4, the system cooling capacity can be calculated as:

$$\dot{Q_{cool}} = \dot{m}(h_4 - h_1) \tag{3}$$

The isentropic power $\dot{W}_{isen}$ can be calculated by:

$$\dot{W}_{\text{isen}} = \frac{\gamma}{\gamma-1}\dot{m}R_g T_{suc}[\left(\frac{P_{dis}}{P_{suc}}\right)^{\frac{\gamma-1}{\gamma}} - 1] \quad (4)$$

where γ is the adiabatic index (1.33 for R1234yf), R_g is the gas constant, T_{suc} is the ambient temperature, P_{dis} is the discharge pressure and P_{suc} is the suction pressure. Therefore, by combining the Eq. (2), Eq. (3) and Eq. (4), the enthalpy at point 2 can be calculated thus the discharge temperature.

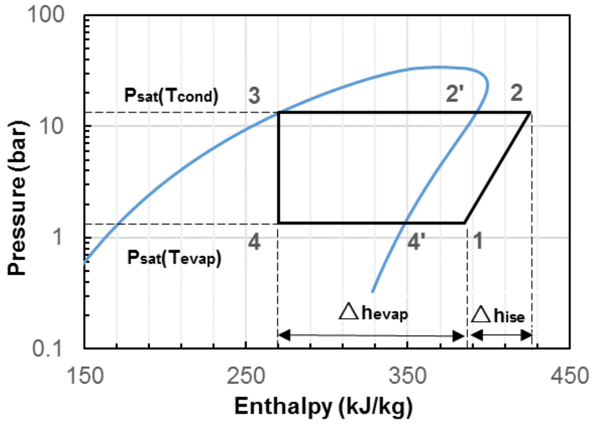

Figure 4 Pressure against enthalpy of linear compressor using R1234yf with fixed evaporator temperature of -23°C and pressure ratio of 10

Assuming the motor efficiency is 86%, the COP of R1234yf by simulation can reach 3.02 with fixed condenser outlet temperature at 50 °C, a pressure ratio of 2.5, a stroke of 12 mm which is 10% lower than the previous experimental result of R134a. This may due to the lower enthalpy of R1234yf.

2.5 Clearance Leakage and Bleed Flow

An oil-free linear compressor cannot achieve a clearance between piston and cylinder as small as that of a traditional compressor with lubricating oil. Leakage across the clearance to compressor body results in imbalance between body pressure and cylinder pressures and this causes the piston offset as the mean position that the piston oscillates about will change. This phenomenon will lead to a reduction of the effective compressor stroke and damage of the compressor if piston hits the cylinder head without control of the piston offset. The leakage across the radial clearance can be recirculated to the compressor suction by adding a bleed flow (shown in Fig. 2).). For a narrow annulus, the volumetric flow rate can be written as below:

$$\dot{V} = \frac{\pi D c^3 dp}{12\mu dx} \quad (5)$$

Where μ is viscosity, c is radial gap.

Thus, by combining the idal gas law, as proposed by Liang et al., (2018) the mass flow rate can be rewritten as:

$$\dot{m} = \frac{\pi D c^3 (P_1+P_2)}{24\mu L R_g T_0}(P_1 - P_2) \quad (6)$$

where P_2 is body pressure, P_1 is inlet pressure and T_0 is inlet temperature, the power loss due to leakage can be written as

$$\dot{W} = \frac{\pi D c^3}{24\mu L}(P_1^2 - P_2^2)[\frac{(P_1-P_2)}{P_1}] \quad (7)$$

2.6 Resonant Frequency

As has been mentioned by Liang et al., (2016), the total stiffness k of the linear compressor is comprised by mechanical spring stiffness k_m and effective spring stiffness k_g. The effective nonlinear spring stiffness of the gas in the compression chamber is given by

$$k_g = (\int PdV - \frac{W_{\text{shaft}}}{2})\frac{2}{S^2} \quad (8)$$

Thus, the resonant frequency f can be calculated as

$$f = \frac{1}{2\pi}\sqrt{\frac{k_g + k_m}{m}} \tag{9}$$

where m is the moving mass given in Table 1.

3. RESULTS AND DISCUSSIONS

3.1 *P-T* Diagram

Fig. 5 shows the saturation pressure as a function of temperature for four different refrigerants based on the data from DuPont (2010, 2003, 2017, 2017). It can be seen that R717 has the highest saturation pressure at same temperature while R600a having the lowest saturation pressure. Thus, the compressor for R717 needs to provide much higher pressure than other three refrigerants, which may increase the production cost. R1234yf and R134a share a similar curve that is between R717 and R600a. Therefore, the replacement of R134a by R1234yf can avoid a comprehensive modification that can be difficult and expensive. Generally, R600a can have lower pressure ratios compared with R1234yf and R134a but the main disadvantages are high flammability and specific compressor displacement.

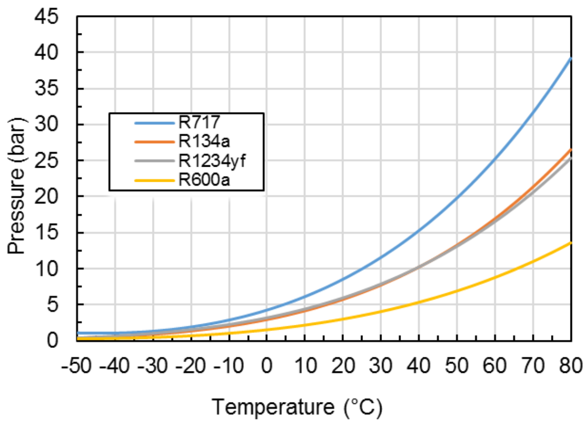

Figure 5 Saturation pressure against temperature of four refrigerants (R717, R134a, R1234yf and R600a)

3.2 *P-V* Diagram

Fig. 6 shows the *P-V* diagram of the linear compressor using R1234yf with fixed evaporator temperature of -23°C, pressure ratio of 10, stroke of 14 mm and dead volume of 226.6 mm^3. This gives a condenser temperature of 55 °C. Process 1-2 is compression process which is assumed to be an isentropic process. Process 3-4 is expansion process. However, the actual cylinder pressure can be affected by the heat transfer through cylinder wall. 2-3 and 4-1 are discharge and suction process, respectively, and the pressure drop has been ignored. However, there is always pressure drop across the discharge and suction valves. The modelling of the valves will improve the accuracy of the model.

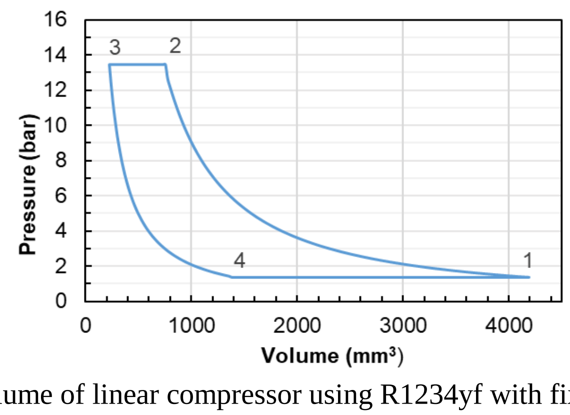

Figure 6 Pressure against volume of linear compressor using R1234yf with fixed evaporator temperature of -23°C, pressure ratio of 10, stroke of 14 mm and dead volume of 226.6 mm^3

3.3 Mean Cylinder Pressure and Shaft power

Fig. 7 shows the shaft power and cylinder mean pressure against different pressure ratios. Both of them increase with the increase of pressure ratio. High pressure ratio provides higher discharge pressure and acquires higher shaft force to deliver the refrigerant. The increase of cylinder mean pressure could lead to higher leakage across the radial gap, which will increase the piston offset (drift).

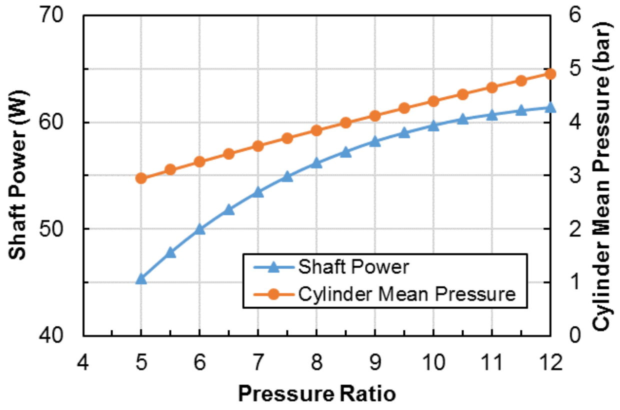

Figure 7 Shaft power and cylinder mean pressure against pressure ratio of linear compressor using R1234yf with fixed evaporator temperature of -23°C

3.4 Bleed Flow

Fig. 8 illustrates the variation of mean bleed flow with different pressure ratios assuming radial clearance of 12.5 µm. The result shows that the bleed flow rate is 5% of main flow. As can be seen, with the increase of the pressure ratio, the bleed flow rate increases. In addition, a similar trend also can be found on clearance power loss in Fig. 8. As mentioned above, the power loss can be expressed as a function of bleed flow rate. Therefore, high pressure ratio leads to an increase of the bleed flow and a reduction of the compressor efficiency. At pressure ratio of 10, the clearance seal power loss represents 8.3% of shaft power.

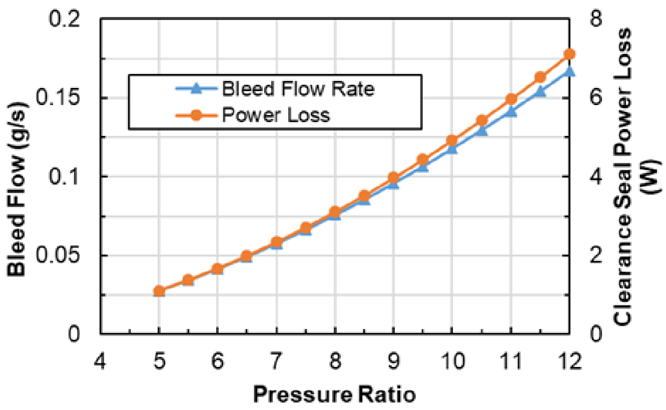

Figure 9 Bleed flow and clearance seal power loss against pressure ratio of linear compressor using R1234yf with fixed evaporator temperature of -23°C and radial clearance of 12.5 µm

Based on Eq. (7), the most effective method to reduce the clearance seal power loss is the reduction of radial clearance. The bleed flow can be reduced by 50% when the radial clearance is 1µm, which is negligible compared with main flow. Therefore, minimising the clearance can be an effective way to enhance the compressor efficiency but this will increase the frictional loss as well. This also shows that using lubricating oil has advantage over oil-free operation.

3.5 Resonant Frequency

Fig. 10 shows the compressor resonant frequency against different pressure ratios with the initial operating frequency of 50 Hz. The input current will be minimised when linear compressor operates at its resonant frequency for each operating condition. As can be seen, with the increase of pressure ratio from 5 to 12, the resonant frequency rises at the same time from 32.7 Hz to 35.3 Hz of the resonant frequency does not change very much with the change of pressure ratio. This indicates that the selection of resonant frequency does not need to be accurate across the range of operating conditions of the linear compressor using R1234yf.

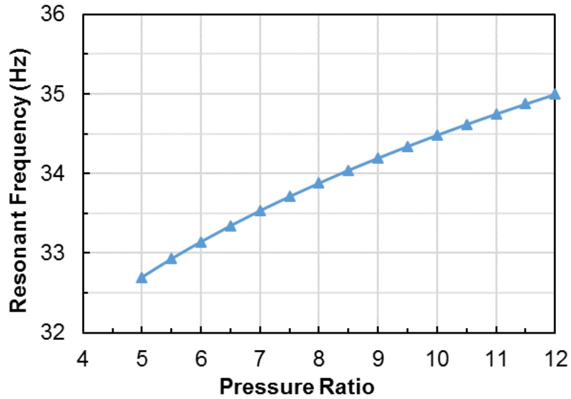

Figure 10 Resonant frequency against pressure ratio of linear compressor using R1234yf with fixed evaporator temperature of -23°C

4. Conclusion and Future Work

R1234yf can be seen as one of the best alternative refrigerants for R134a for their similar thermodynamic property. Oil-free linear compressor can be an ideal option for R1234yf, which can be used in the refrigerator and mobile air conditioner. The mathematical model for this work predicts the performance of a prototype oil-free linear compressor using R1234yf. Key findings are listed below:

(1) The bleed flow rate is about 5% of that of the main flow.

(2) The resonant frequency rises slightly with the increase of pressure ratio. The recommended operating frequency for the compressor is 34 Hz.

(3) The bleed flow and power loss increase with the increase of pressure ratio. At pressure ratio of 10, and clearance seal power loss represents 8% of shaft power.

(4) Cylinder mean pressure increase with the increase of pressure ratio, which lead to higher piston offset.

(5) COP of R1234yf is around 10% lower than the experiment result of R134a with fixed condenser temperature of 50 °C, pressure ratio of 2.5, stroke of 12 mm.

The future work will focus on instrumenting the prototype oil-free linear compressor with R12434yf. The experimental data will then be compared with simulation data from this work.

ACKNOWLEDGEMENT

The authors are very grateful to Prof Richard Stone, Dr Mike Dadd and Mr Paul Bailey at the University of Oxford for the prototype oil-free linear compressor. The Research Development Fund from the University of Sussex (UA016-05) for supporting the instrumentation of the linear compressor is also acknowledged.

NOMENCLATURE

p	pressure (bar)	R_g	gas constant (0.0729 kJ*kg^{-1}*K^{-1})
T	temperature (°C)	V	molar volume (mol·L^{-1})
μ	Viscosity (uPa*s)	c	radial gap (μm)
D	Piston diameter (mm)	f	Operating frequency (Hz)
$\dot{m}$	Mass flow rate (g/s)	L	Piston Length (mm)
γ	Adiabatic index		

References

Richter, M., McLinden, . M. O. & Lemmon, E. W., 2011. Thermodynamic Properties of 2,3,3,3-Tetrafluoroprop-1-ene (R1234yf): Vapor Pressure and p-ρ-T Measurements and an Equation of State. *Journal of Chemical and Engineering Data,* 56(7), pp. 3254-3264.

Del Col, D., Torresin, D. & Cavallini, A., 2010. Heat transfer and pressure drop during condensation of the low GWP refrigerant R1234yf. *International Journal of Refrigeration,* 33(7), pp. 1307-1318.

Dupont, 2003. *Thermodynamic Properties of HFC-134a.* [Online] Available at: http://www.pfri.uniri.hr/~pkralj/R134a_thermo_prop_si.pdf [Zugriff am 29 January 2018].

Dupont,2010.*Thermodynamic Properties of Dupont R1234yf.* [Online]
Available at:
https://www.chemours.com/Refrigerants/en_US/assets/downloads/k24239_Opteon_yf_thermo_properties_SI.pdf
[Zugriff am 10 January 2017].

Government, U., 2014. *Guidance bans on F gas in new equipment.* [Online] Available at: https://www.gov.uk/guidance/bans-on-f-gas-in-new-equipment [Zugriff am 29 January 2018].

Lee , Y. & Jung, D., 2012. A brief performance comparison of R1234yf and R134a in a bench tester for automobile applications. *Applied Thermal Engineering,* Band 35, pp. 240-242.

Lenz, J. R., 2002. *Polytropic Exponents for Common Regrigerants.* West Lafayette, s.n.

Liang , K. et al., 2014. Comparison between a crank-drive reciprocating compressor and a novel oil-free linear compressor. *International Journal of Refrigeration,* Band 45, pp. 25-34.

Liang, K., 2018. Analysis of oil-free linear compressor operated at high pressure ratios for household refrigeration. *Energy,* Band 151, pp. 324-331.

Liang, K., Stone, R., Dadd, M. & Bailey, P., 2016. Piston position sensing and control in a linear compressor using a search coil. *International Journal of Refrigeration,* June, pp. 32-40.

Liang, K. et al., 2014. Modelling and measurement of a moving magnet linear compressor performance. *Energy,* Band 66, pp. 487-495.

Navarro-Esbrí, J. et al., 2013. Experimental analysis of R1234yf as a drop-in replacement for R134a in a vapor compression system. *international journal of refrigeration,* 36(3), pp. 870-880.

pump,I.h.,2017.*R600a(Iso-butane).*[Online]
Available at: http://www.industrialheatpumps.nl/server/multimediaserve/167
[Zugriff am 29 January 2018].

pump,I.h.,2017.*R717(Ammonia).*[Online]
Available at: http://www.industrialheatpumps.nl/server/multimediaserve/168
[Zugriff am 29 January 2018].

Zilion, C., Brown, J. S., Schiochet, G. & Cavallini, A., 2011. The refrigerant R1234yf in air conditioning systems. *Energy,* 36(10), pp. 6110-6120.